GROUND DATA PROCESSING & PRODUCTION OF THE LEVEL 1 HIGH RESOLUTION MAPS

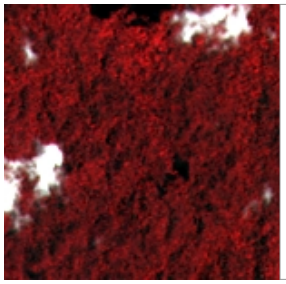

VALERI 2002

COUNAMI site
(tropical forest)

Philippe Rossello, Marie Weiss, Frédéric Baret

November 2005

CONTENTS

1. Introduction

This report describes the production of the high resolution, level 1, biophysical variable maps for the Counami site in 2002 (see campaign report for more details about the site and the ground measurement campaign: annex 1 or http://www.avignon.inra.fr/valeri). Level 1 map corresponds to the map derived from the determination of a transfer function between reflectance values of the SPOT image acquired during (or around) the ground campaign, and biophysical variable measurements (hemispherical images). For each Elementary Sampling Unit (ESU), the hemispherical images were processed using the CAN-EYE software (Version 3.4) developed at INRA-CSE. The derived biophysical variable maps are:

• four Leaf Area Index (LAI) are considered: effective LAI (LAIeff) and true LAI (LAItrue) derived from the description of the gap fraction as a function of the view zenith angle; effective LAI57 (LAI57eff) and true LAI57 (LAI57true) derived from the gap fraction at 57.5°, which is independent on the leaf inclination. Effective LAI and effective LAI57 do not take into account clumping effect. LAItrue and LAI57true are derived using the method proposed by Lang and Yueqin[1] (1986);

• cover fraction (fCover): it is the percentage of soil covered by vegetation. To improve the spatial sampling, fCover was computed over 0 to 10° zenith angle;

• fAPAR: it is the fraction of Absorbed Photosynthetically Active Radiation (PAR=400-700nm). The fAPAR is defined either instantaneously (for a given solar position) or integrated all over the day. Following a study based on radiative transfer model simulations, it has been shown that the root mean square error between instantaneous fAPAR computed every 30 minutes and the daily fAPAR is the lowest for instantaneous fAPAR at 10h00 AM (solar time, RMSE = 0.021). Therefore, the derivation of fAPAR from CAN-EYE corresponds to the instantaneous black sky fAPAR at 10h00 AM.

The Counami site is covered by the tropical rain forest. It is a large flat plain. The canopy around 20 m high is very dense and the understorey is generally dense. The detailed description of the site is available (http://www.avignon.inra.fr/valeri) in the report on measurement campaign (09/2001).

The site coordinates are described in Table 1:

	UTM, 22 North, WGS84 (units = meters)		Geographic Lat/Lon WGS84 (units = degrees)	
	Northing	Easting	Lat.	Lon.
Upper left corner	592601.0860	250589.1750	5.35715216	-53.25058693
Lower right corner	589561.0860	253589.1750	5.32977048	-53.22343084
Center	591081.0860	252109.1750	5.34346226	-53.23682821

Table 1. Description of the site coordinates.

The ground measurements were carried out from 2002/10/07 to 2002/10/18, while the high spatial resolution image (SPOT4, HRVIR1, resolution: 20 m) was acquired on 2002/10/01.

2. Available data

2.1. SPOT Image

The SPOT image was acquired the 1st October 2002 by HRVIR1 on SPOT4 and few clouds are present in the image. It was geo-located by SPOTimage (SPOTView basic). The projection is UTM 22 North, WGS-84 (please, refer to the campaign report for more details: annex 1 or http://www.avignon.inra.fr/valeri).

Figure 1 shows the relationship between Red and near infrared (NIR) SPOT channels. The different colours correspond to the three classes determined by the non supervised classification based on NDVI (§2.3.3). The highest values in the NIR and the Red correspond to the reflectance of the clouds (green class) which cover 4.2 % of the image (Figure 4). The cloud class will not be taken into account in the derivation of the biophysical variable maps from the image (no data available in the cloud mask). Note that for a tropical forest, the NIR value

[1] Lang, A.R.G. and Yueqin, X., 1986. Estimation of leaf area index from transmission of direct sunlight in discontinuous canopies. Agric. For. Meteorol., 37: 229-243.

appears to be quite low (<0.3) and that the range in the NIR corresponding to low values in the Red domain is quite significant (0.07 to 0.25).

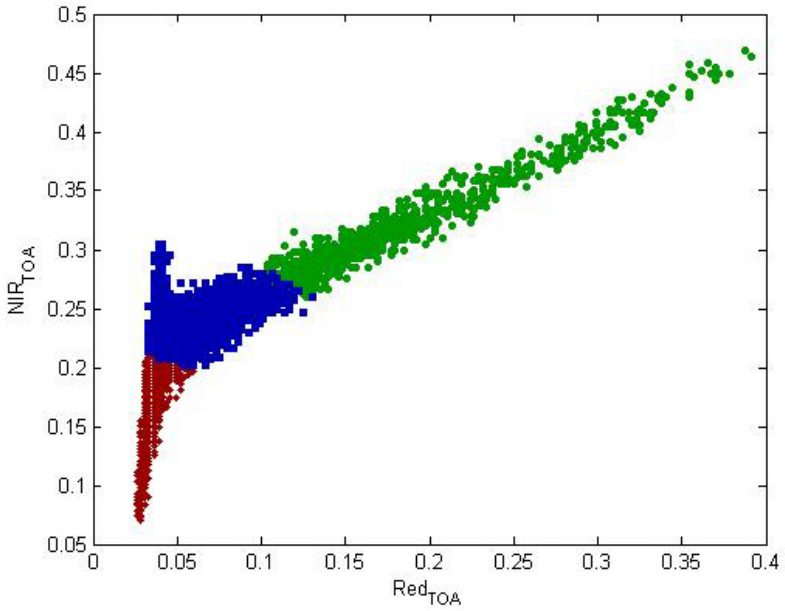

Figure 1. Red/NIR relationship on the SPOT image for Counami, 2002.

2.2. Hemispherical images

The hemispherical images were processed using the CAN-EYE software (Version 3.4) to derive the biophysical variables. Figure 2 and Figure 3 show the distribution of the several variables over the sampled ESUs. As there was understorey on five ESUs (L1b, L2b, L4b, L5b, L6b), hemispherical images were acquired from above the understorey and from below the canopy (trees). The two sets of acquisition were processed separately to derived LAI (effective and true), LAI57 (effective and true), fCover, and fAPAR. The ESU biophysical variable was then computed as:

- LAIeff, LAI57eff, LAItrue, LAI57true: LAI(above) + LAI(below).
- fCover: 1-(1-fCover(above))*(1-fCover(below)). This assumes that independency of the gaps inside the understorey and the gaps inside the trees which is not true at all the scales but it is the only way to get the total fCover. However, for the local scales considered, this might be true as a first order approximation.
- fAPAR: 1-(1-fAPAR(below))*(1-fAPAR(above)), since 1-fAPAR can be considered equivalent to a gap fraction. Here again, the same independency between the two layers has to be assumed.

Note that LAI (effective and true) derived from directional gap fraction and LAI derived from gap fraction at 57.5° (effective and true) are consistent (Figure 2 and Figure 3). Effective LAI (LAIeff, LAI57eff) varies from 2.6 to 4, while true LAI (LAItrue, LAI57true) varies from 3.45 to 5.9. This range shows a homogeneous site in terms of LAI. For values, LAIeff and LAI57eff are lower than LAItrue and LAI57true. This is due to the clumping observed for several ESUs. The relationship between fAPAR and LAI is in agreement with what is expected (Beer-Lambert law) while the fCover-LAI relationship is more noisy. Note that the fCover and fAPAR values are very high: fCover from 0.76 to 0.93 and fAPAR from 0.84 to 0.93.

To build the relationships between biophysical variables and SPOT data, the reflectance of a given forest ESU was considered as the average reflectance over the central pixel + the 8 surrounding pixels. This takes into account the fact that the height of the trees are about 20 m and consequently the fish-eye observes an area of $\pi \times [20 \times \tan(60°)]^2 \cong 3750$ m², *i.e.* close to the area of 9 SPOT pixels (=3600m²) when using a maximum view zenith angle of 60°.

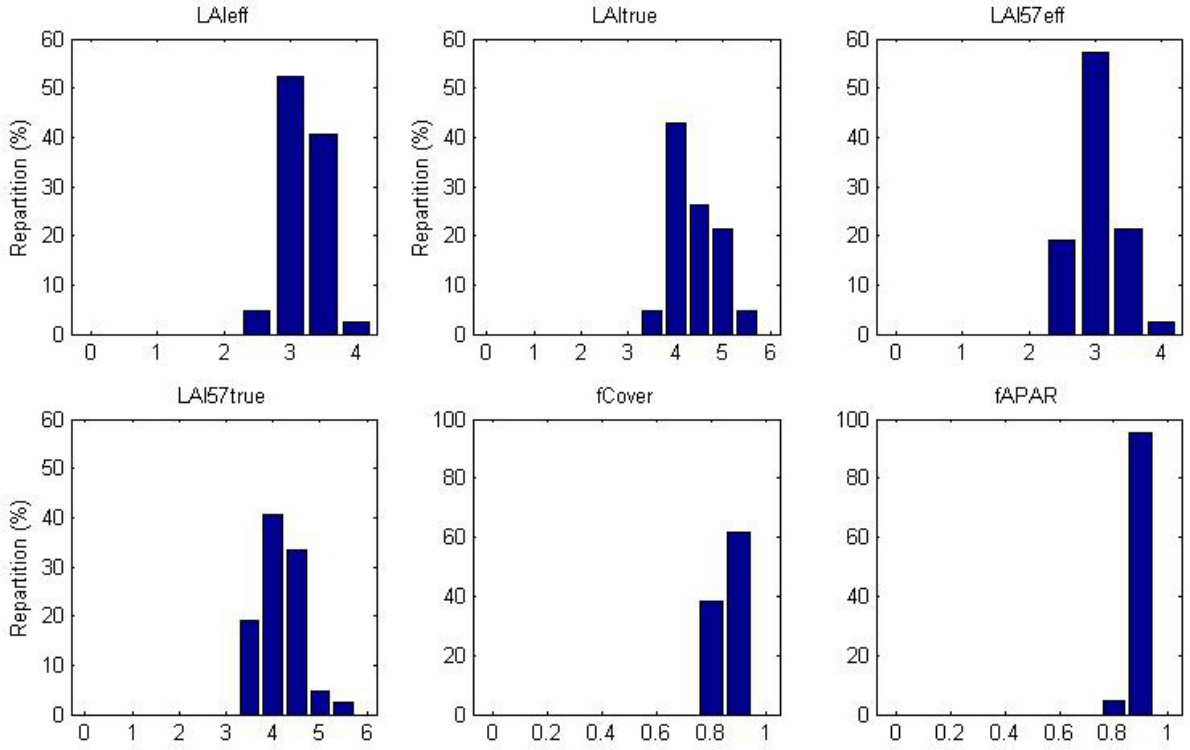

Figure 2. Distribution of the measured biophysical variables over the ESUs.

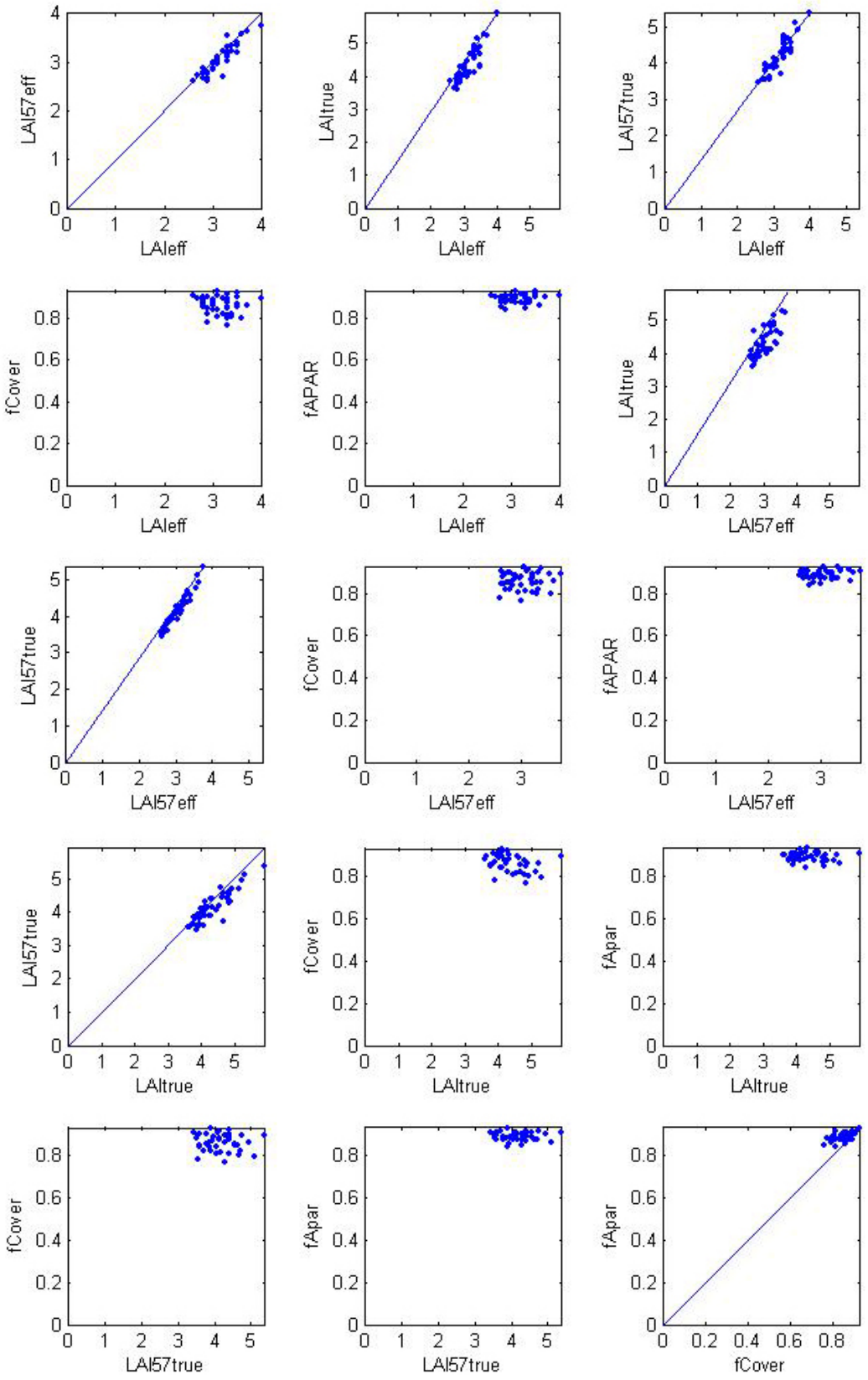

Figure 3. Relationships between the different biophysical variables

2.3. Sampling strategy

2.3.1. Principles

The sampling strategy is defined in the report on measurement campaign (please read the annex 1). The distribution of the ESUs is mainly designed empirically and the sampling of each ESU is based on twelve elementary photographs.

Figure 4 shows that the 42 ESUs are evenly distributed over the site (3 x 3 km). The processing of the ground data has shown that G2 (in black on Figure 4) was located under a cloud. This ESU was eliminated.

Finally 41 ESUs have been kept for the computation of the transfer function.

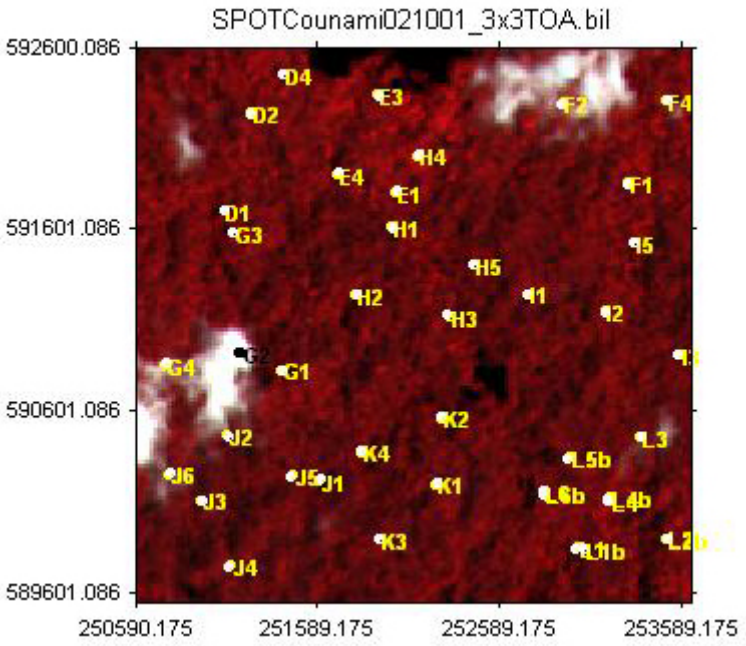

Figure 4. Distribution of the ESUs around the Counami site. ESU in black (G2) was eliminated for the computation of the transfer function.

2.3.2. Evaluation based on NDVI values

The sampling strategy is evaluated using the SPOT image by comparing the NDVI distribution over the site with the NDVI distribution over the ESUs (Figure 5). As the number of pixels is drastically different for the ESU and whole site (WS = 22500 in case of a 3 x 3 km SPOT image at 20 m resolution), it is not statistically consistent to directly compare the two NDVI histograms. Therefore, the proposed technique consists in comparing the NDVI cumulative frequency of the two distributions by a Monte-Carlo procedure which aims at comparing the actual frequency to randomly shifted sampling patterns. It consists in:

1. computing the cumulative frequency of the *N* pixel NDVI that correspond to the exact ESU locations;
2. then, applying a unique random translation to the sampling design (modulo the size of the image);
3. computing the cumulative frequency of NDVI on the randomly shifted sampling design;
4. repeating steps 2 and 3, 199 times with 199 different random translation vectors.

This provides a total population of $N = 199 + 1$(actual) cumulative frequency on which a statistical test at acceptance probability $1 - \alpha = 95\%$ is applied: for a given NDVI level, if the actual ESU density function is between two limits defined by the $N\alpha/2 = 5$ highest and lowest values of the 200 cumulative frequencies, the hypothesis assuming that WS and ESU NDVI distributions are equivalent is accepted, otherwise it is rejected.

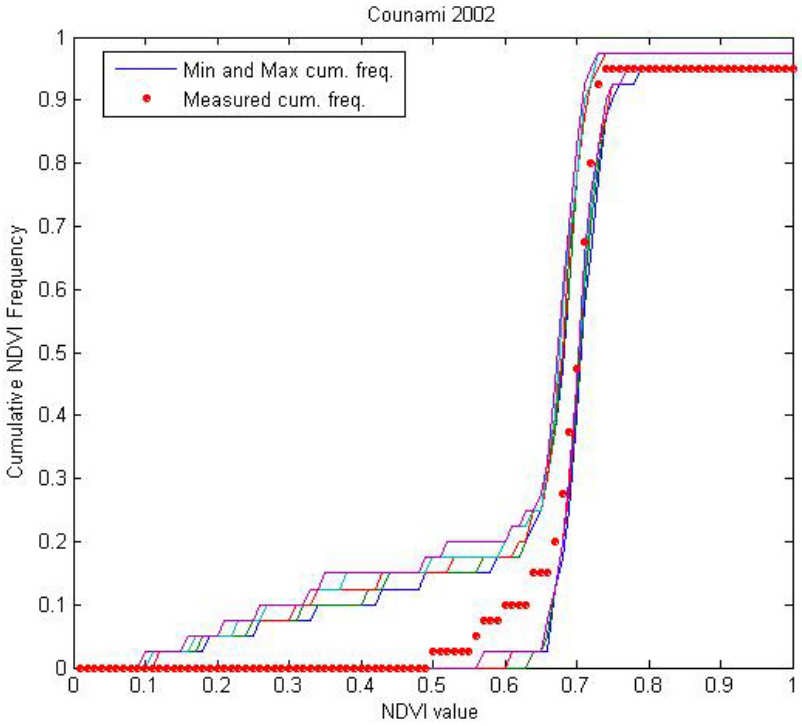

Figure 5. Comparison of the ESU NDVI distribution and the NDVI distribution over the whole image.

Figure 5 shows that the NDVI distribution of the 41 ESUs is quite good over the whole site (comprised between the 5 highest and lowest cumulative frequencies) even if the cumulative frequency curve is often close to the boundaries for high NDVI values. It reaches even the boundaries on several occasions. Note that NDVIs lower than 0.50 have not been sampled although they are present in the image. NDVIs lower than 0.14 which have not been sampled during the campaign correspond to clouds. Moreover, the site is homogeneous in terms of NDVI since the highest and lowest distributions are close.

2.3.3. Evaluation based on classification

A non supervised classification based on the k_means method (Matlab statistics toolbox) was applied to the reflectance of the SPOT image to distinguish if different behaviours on the image for the biophysical variable-reflectance relationship exist.

A number of 3 classes was chosen (Figure 6). The distribution of the classes on the image and on the ESUs is similar. The class 2 is not represented because the ESU G2 was eliminated. It corresponds to clouds. Class 3 is under-represented while class 1 appears to be over-sampled.

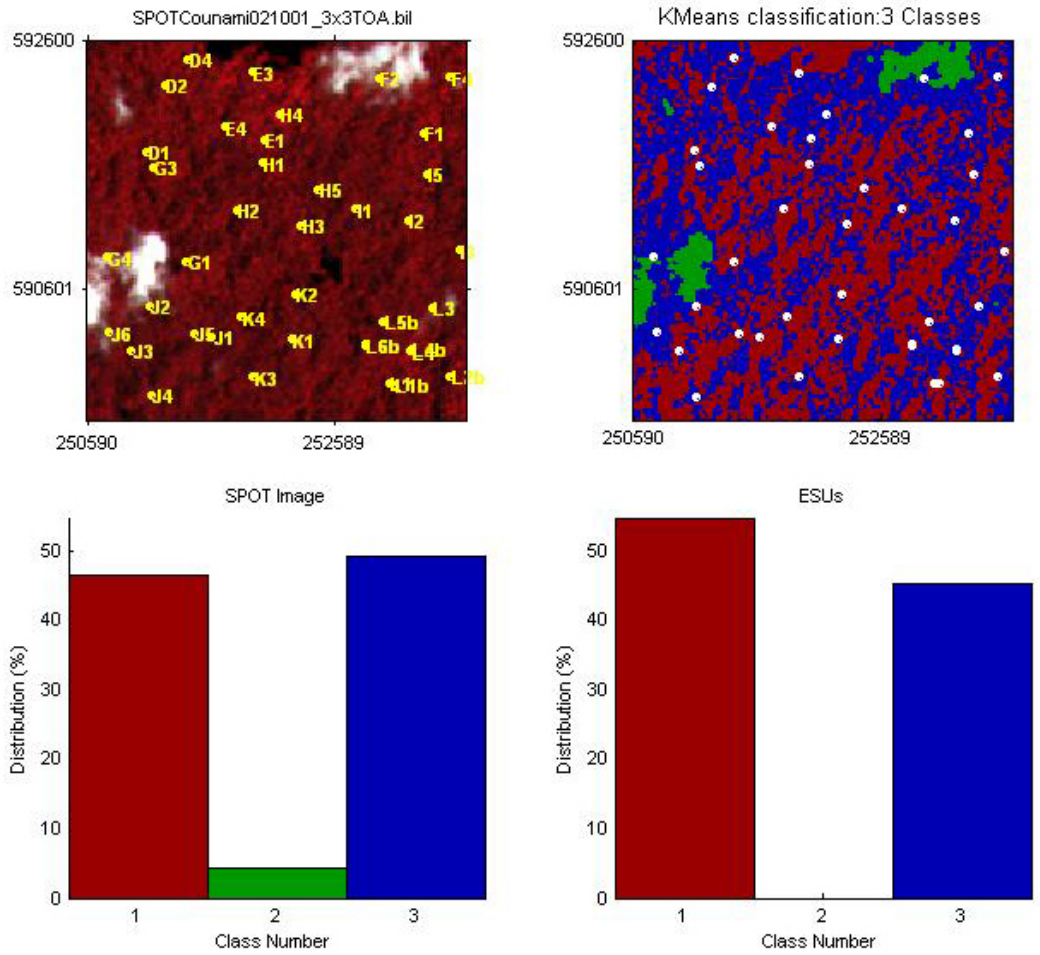

Figure 6. Classification of the SPOT image. Comparison of the class distribution between the SPOT image and sampled ESUs.

Figure 7 shows the different relationships observed between the biophysical variables and the corresponding NDVI on the ESUs, as a function of the SPOT classes determined from non supervised classification.

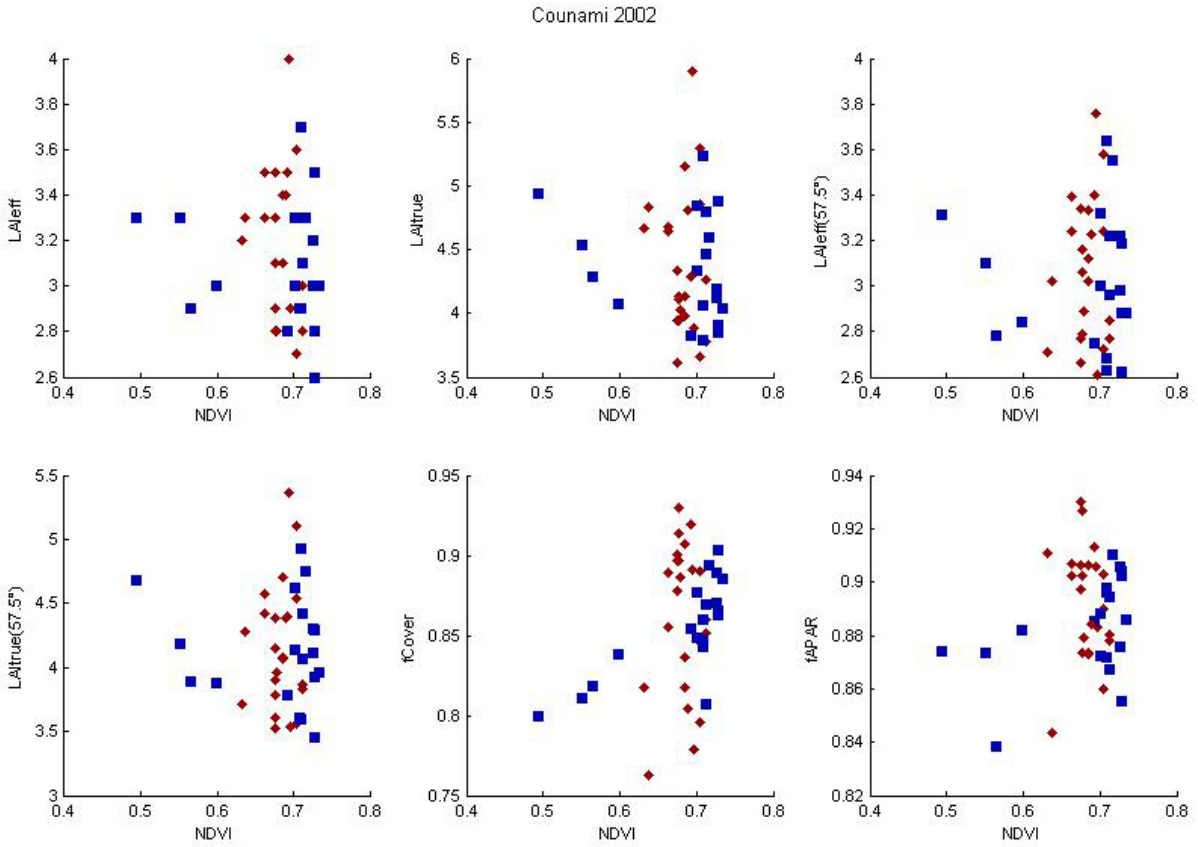

Figure 7. NDVI-Biophysical Variable relationships as a function of SPOT classes

There is no relation between NDVI and biophysical variables due to the fact that the reflectance is saturating for high LAI values. For classes 1 and 3, one behaviour can be observed even if some points differ. These two classes (41 ESUs) correspond to the tropical forest. Therefore, a single transfer function per variable will be generated. A default value (-0.001) will be attributed to the pixels corresponding to the clouds.

2.3.4. Using convex hulls

A test based on the convex hulls was also carried out to characterize the representativeness of ESUs. Whereas the evaluation based on NDVI values uses two bands (red and NIR), this test uses the four bands of the SPOT image. A flag image, is computing over the reflectances (Figure 8). The result on convex-hulls can be interpreted as:

- pixels inside the 'strict convex-hull': a convex-hull is computed using all the SPOT reflectance corresponding to the ESUs belonging to the class. These pixels are well represented by the ground sampling and therefore, when applying a transfer function the degree of confidence in the results will be quite high, since the transfer function will be used as an interpolator;
- pixels inside the 'large convex-hull': a convex-hull is computed using all the reflectance combination (±5% in relative value) corresponding to the ESUs. For these pixels, the degree of confidence in the obtained results will be quite good, since the transfer function is used as an extrapolator (but not far from interpolator);
- pixels outside the two convex-hulls: this means that for these pixels, the transfer function will behave as an extrapolator which makes the results less reliable. However, having a priori information on the site may help to evaluate the extrapolation capacities of the transfer function.

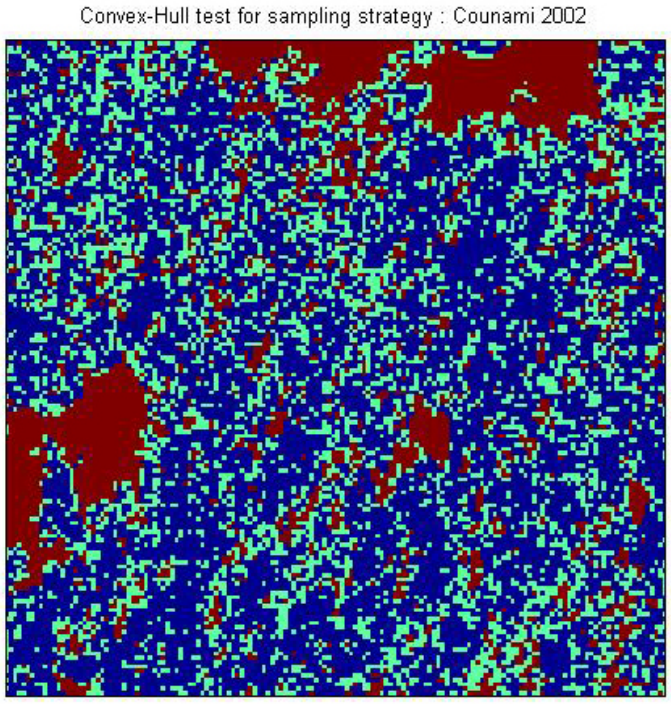

Figure 8. Evaluation of the sampling based on the convex hulls. The map is shown at the bottom: blue and light blue correspond to the pixels belonging to the 'strict' and 'large' convex hulls and red to the pixels for which the transfer function is extrapolating.

This map shows that the pixels inside the 'strict convex-hull' and the 'large convex-hull' are numerous. They correspond to a very homogeneous land cover (tropical forest). The number of pixels outside the two convex-hulls is rather low: the clouds and the area in the shade where the biophysical variable can not be estimated are in question. The representativeness of the ESUs is thus very good.

3. Determination of the transfer function for the four biophysical variables: LAIeff, LAItrue, LAI57eff, LAI57true, fCover, fAPAR

3.1. The transfer functions considered

Three types of transfer functions are usually tested in the frame of the VALERI project:

- AVE: if the number of ESUs belonging to the class is too low. The transfer function consists only in attributing the average value of the biophysical variable measured on the class to each pixel of the SPOT image belonging to the class.

- REG: if the number of ESUs is sufficient, multiple robust regression between ESUs reflectance (or Simple Ratio) and the considered biophysical variable can be applied: we used the 'robustfit' function from the matlab statistics toolbox. It uses an iteratively re-weighted least squares algorithm, with the weights at each iteration computed by applying the bisquare function to the residuals from the previous iteration. This algorithm provides lower weight to ESUs that do not fit well. The results are less sensitive to outliers in the data as compared with ordinary least squares regression. At the end of the processing, three errors are computed: classical root mean square error (RMSE), weighted RMSE (using the weights attributed to each ESU) and cross-validation RMSE (leave-one-out method).

- LUT: if the number of ESUs is sufficient, Look-Up-Tables are also enviewed: a look-up table is built using ESUs reflectances and the corresponding measured biophysical variable. For a given pixel, a cost function is computed as the sum of the square difference between the pixel reflectances and the ESU reflectances over the 4 bands, divided by the standard deviation computed on ESU reflectances. The result of the cost function is sorted in ascending order, and the biophysical variable estimated for the given pixel is computed as the mean value of the first *n* ESUs providing the lowest value of the cost function. Different values of *n* are considered to get the lowest cost function. This method is reliable only if the ESU NDVI distribution is quite comparable with the whole site NDVI distribution, which was quite the case for this Counami site.

As there is no evident relationship between NDVI and LAI (§2.3.3), the results of the multiple robust regression (REG) and the Look-Up-Tables (LUT) did not show pertinent results. Therefore, even if the number of ESUs belonging to the classes is sufficient, the 'AVE' method is applied. For each class determined in §2.3 (classes 1 and 3), the transfer function consists only in attributing the average value of the biophysical variable measured on the class to each pixel of the SPOT image belonging to the class.

3.2. Results

Following, the results of the transfer function:

	LAIeff	LAItrue	LAI57eff	LAI57true	fCover	fAPAR
Class 1	3.187	4.389	3.072	4.163	0.862	0.893
Class 2 (clouds)	*-0,001*	*-0,001*	*-0,001*	*-0,001*	*-0,001*	*-0,001*
Class 3	3.100	4.357	3.029	4.137	0.855	0.883

Table 2. Transfer function applied to the whole site for the different biophysical variables

The values of biophysical variable maps are thus very homogeneous with close values between class 1 and class 3. The class 2 values correspond to clouds: a default value (-0.001) is attributed to the pixels belonging to this class.

Note that the average value of the ESUs values per biophysical variable over the whole Counami site is also representative:

LAIeff.ESU = 3.1476; LAItrue.ESU = 4.3742; LAI57eff.ESU = 3.0526; LAI57true.ESU = 4.1514; fCover.ESU = 0.8586; fAPAR.ESU = 0.8883.

4. Conclusion

The transfer function is obtained by using 41 ESUs. The Counami site is homogeneous in terms of LAI and NDVI. However, note that no relationship exists between these two variables. Therefore, the selected transfer function consists in attributing the average value of the biophysical variable measured on the class to each pixel

of the SPOT image belonging to the class. The average value of the ESUs per biophysical variable over the whole site is also representative and consistent with the obtained maps (§3.2).

The Counami site is particular in so far as the estimation of biophysical variables above the tropical forests is difficult. The heterogeneity of the landscape could not be accurately evaluated because of the saturation of the signal due to high LAI values.

The biophysical variable maps are available in UTM, 22 North, projection coordinates (Datum: WGS-84) at 20m resolution.

5. Acknowledgements

We thank people who participated to the field experiment: **Valéry Gond** (IRD, Cayenne, French Guyana), **Jean-François Hanocq** (INRA, Avignon), **Pétrus Naisso, Ficadici Kago, Étienne Abner** and **Pierre-Marie Pidoux** (CIRAD, Montpellier).

ANNEXES

Annex 1

Ground measurement acquisition report for the VALERI site **Counami**

sampled from 07/10/2002 to 18/10/2002

Gond Valéry
Organization: CIRAD
email: gond@cayenne.ird.fr

Date of report 19/10/2002

People participating to the field experiment:

Fistname & Name	0rganization
HANOCQ Jean-François	INRA
NAISSO Pétrus	CIRAD
KAGO Ficadici	CIRAD
ABNER Etienne	CIRAD
PIDOUX Pierre-Marie	CIRAD

Site coordinates

	Lat-Long WGS84 (Deg min.00)		UTM / WGS84 UTM 22		Other projection*	
	Lat.	Long.	Easting	Northing		
Upper left corner	5.35714271	-53.2504893	250600	592600		
Lower right corner	5.33012260	-53.2233348	253600	589600		

All the projections characteristics are provided in the following table (see http://www.avignon.inra.fr/valeri/, methodology page, GPS document for more information).

Ground control points

Name	Team	Month	Day	Hour	Minute	Easting(m)	Northing(m)
GCP1	D	10	24	10	35	257051	596529
GCP2	D	10	24	11	28	253727	590013
GCP3	D	10	24	12	15	249996	585594
GCP4	D	10	24	12	39	249534	585422

*This is extracted from the Excel file GPSCounami2002.xls

Description of the site and land cover

Category according to IGBP classification

Evergreen Broadleaf forest.

Comments on the land cover

Tropical rain forest.

Topography

Hilly.

Spatial Sampling scheme

Sensors used for sampling the ESUs

	Method	Comments
☒	Hemispherical photographs	Mainly upward. A test on downward photo in 5 plots.
☐	LAI2000	
☐	TRAC	
☐	Ceptometer	
☐	Direct measurements	
☐	Other	

Sampling strategy for the ESU

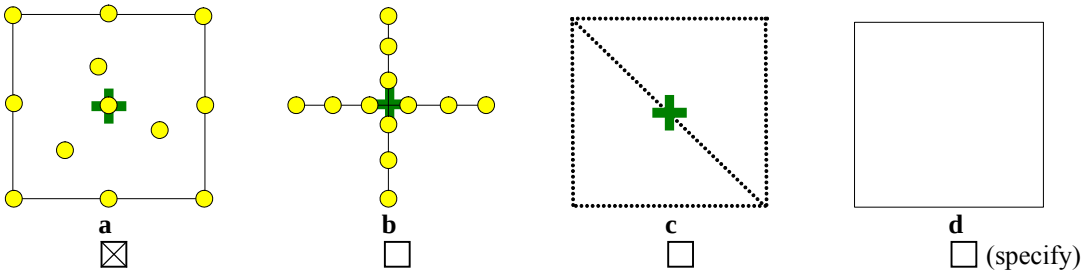

The high spatial resolution image

Satellite

Satellite used	SPOT4, HRVIR1
Level of processing	2B
Projection type	UTM/WGS84

List of the ESUs

This is extracted from the Excel file GPSCounami2002.xls

Name	Team	Month	Day	Hour	Minute	Easting(m)	Northing(m)
ULC						250600	592600
LRC						253600	589600
D1	B	10	10			251083	591700
D2	B	10	10	10	25	251229	592230
D3	B	10	10	11	6	251284	592591
D4	B	10	10	11	34	251411	592438
E1	B	10	9	10	59	252021	591796
E2	A	10	10			252451	592591
E3	B	10	10			251926	592331
E4	B	10	10	14	15	251702	591897
F1	A	10	10			253295	591850
F2	A	10	10			252938	592285
F3	A	10	10			253180	592797
F4	A	10	10			253504	592295
G1	B	10	8	9	29	251400	590823
G2	B	10	8	10	13	251178	590916
G3	B	10	10	9	42	251130	591573
G4	B	10	8			250762	590852
H1	B	10	9			252003	591607
H2	B	10	9			251800	591234
H3	B	10	9	10	41	252314	591112
H4	B	10	9			252144	591997
H5	B	10	9	12	3	252452	591395
I1	A	10	9			252752	591240
I2	A	10	9	10	48	253168	591147
I3	A	10	9	9	47	253579	590910
I4	A	10	9			253636	590990
I5	A	10	9			253324	591522
J1	B	10	7			251600	590217
J2	A	10	8			251100	590467
J3	A	10	8			250960	590110
J4	A	10	8			251117	589750
J5	A	10	8			251459	590247
J6	B	10	8	11	20	250783	590253
K1	AB	10	7	11	47	252240	590197
K2	A	10	7	12	15	252270	590559
K3	B	10	7			251934	589894
K4	B	10	7			251834	590374
L1	C	10	18	11	33	253018	589851
L1b	D	10	18			253054	589838
L2	C	10	18	12	8	253506	589902
L2b	D	10	18			253504	589900
L3	A	10	11			253361	590452
L4	C	10	18	9	49	253192	590100
L4b	D	10	18			253199	510125
L5	C	10	18	10	25	252978	590343
L5b	D	10	18			252975	520343
L6	C	10	18	10	51	252828	590154
L6b	D	10	18			252830	590151

Acknowledgements

Thanks to IRD-Cayenne for sharing vehicles.

Photo gallery

The photos illustrating the campaign are to be stored in the directory “photo gallery” and the labels should be indicated in the table above:

#	File name	Comments
1	Counami_2002_1	Encampment interior
2	Counami_2002_2	Encampment environment
3	Counami_2002_3	Encampment from the garden
4	Counami_2002_4	Encampment from the garden
5	Counami_2002_5	The entrace
6	Counami_2002_6	Road access
7	Counami_2002_7	Tropical mushroom
8	Counami_2002_8	Tropical mushroom from the north
9	Counami_2002_9	Pétrus, Valéry, Kago and Jean-François
10	Counami_2002_10	Valéry, Pétrus, Jean-François and Kago

Annex 2

The methods used by the transfer functions to estimate the biophysical variable values

The previous processes (Table 1) use mainly the multiple robust regression (REG) on reflectance. The LUT method is never selected and the REG method on logarithm of the reflectance is not much used by the transfer functions (http://www.avignon.inra.fr/valeri). In fact, the results using the logarithm of the reflectance are often similar to those using the reflectance. The Table 1 indicates the selected methods for the different VALERI sites:

Warning: the following informations are partial. For more details, please read the complete report of process of the wished site.

				methods			
site	country	date	landcover	AVE*	REG** (ρ=reflectance ; log=logarithm)	LUT ***	comments
Aek Loba	Indonesia	05/2001	plam tree plantation	-	ρ: LAI	-	LAI map retrieved using the linear NIR-LAI relationship
Alpilles	France	03/2001	cropland	-	ρ: LAI	-	only the multiple regression was applied
Alpilles	France	07/2002	crops and grassland	-	ρ: LAIeff,LAItrue,LAI57eff, LAI57true,fCover,fAPAR	-	the transfer function using the log(ρ) creates coplanar points and estimates negative LAI, fCover and fAPAR values; the REG method provides better results in terms of cross-validation RMSE
Barrax	Spain	07/2003	cropland	class 2	ρ: LAI,LAI57,fCover,fAPAR	-	very similar results between REG on ρ and REG on log(ρ) in terms of cross-validation RMSE, but the number of ESUs with weights < 0.7 is higher when using the log(ρ)
Concepción	Chile	01/2003	mixed forest	-	ρ: LAI,LAI57,fAPAR	-	very similar results between REG on ρ and REG on log(ρ), but the number of ESUs with weights < 0.7 is higher when using the log(ρ)
Counami	French Guyana	10/2002	tropical forest	classes 1,3	-	-	no relation between NDVI and biophysical variables; the average value of the ESUs is representative since the Counami site is very homogeneous (class 2=clouds)
Fundulea	Romania	03/2001	crops	-	ρ: LAI	-	only the multiple regression was applied
Fundulea	Romania	06/2003	crops	class 1	ρ: LAI,LAI57,fCover,fAPAR	-	similar results between REG on (ρ) and REG on log(ρ) in terms of cross-validation RMSE
Gilching	Germany	07/2002	crops and forests	-	ρ: LAIeff,LAItrue,LAI57eff, LAI57true,fCover,fAPAR	-	the REG method provides better results in terms of cross-validation RMSE for all the variables; close results between REG on (ρ) and REG on log(ρ)
Haouz	Morocco	03/2003	cropland	-	log(ρ): LAI,LAI57,fCover,fAPAR	-	the number of ESUs with weights < 0.7 is lower using the log(ρ); the LUT method provides systematically higher RMSE value than for REG (weighted RMSE for REG)
Hisikangas	Finland	08/2003	forests	class 5	log(ρ): LAI,fCover	-	the LUT method provides systematically higher RMSE value than for REG
Järvselja	Estonia	06/2003	boreal forest	-	log(ρ): LAI; ρ: fCover	-	the REG method provides better results in terms of cross-validation RMSE; for LAI, the results using the log(ρ) are slightly better; a simple multiple regression was applied for fCover

...

				methods			
site	country	date	landcover	AVE*	REG** (ρ=reflectance ; log=logarithm)	LUT ***	comments
Romilly-sur-Seine	France	07/2000	cropland	-	-	-	LAI map retrieved using collocated kriging
Sud-Ouest	France	07/2002	crops and grassland	-	ρ: LAIeff,LAItrue,LAI57eff, LAI57true,fCover,fAPAR	-	the REG method provides better results in terms of cross-validation RMSE for all the biophysical variables
Turco	Bolivia	04/2003	cropland	-	ρ: LAI,LAI57,fCover,fAPAR	-	very close results between REG on ρ and REG on log(ρ)

*AVE: this method is used if the number of ESUs belonging to the class is too low. The transfer function consists only in attributing the average value of the biophysical variable measured on the class to each pixel of the SPOT image belonging to the class.

**REG: if the number of ESUs is sufficient, multiple robust regression between ESUs reflectance (or Simple Ratio) and the considered biophysical variable can be applied: we used the 'robustfit' function from the matlab statistics toolbox. It uses an iteratively re-weighted least squares algorithm, with the weights at each iteration computed by applying the bisquare function to the residuals from the previous iteration. This algorithm provides lower weight to ESUs that do not fit well. The results are less sensitive to outliers in the data as compared with ordinary least squares regression. At the end of the processing, three errors are computed: classical root mean square error (RMSE), weighted RMSE (using the weights attributed to each ESU) and cross-validation RMSE (leave-one-out method).

***LUT: if the number of ESUs is sufficient, the look-up table is built using ESUs reflectances and the corresponding measured biophysical variable. For a given pixel, a cost function is computed as the sum of the square difference between the pixel reflectances and the ESU reflectances over the 3 or 4 bands, divided by the standard deviation computed on ESU reflectances. The result of the cost function is sorted in ascending order, and the biophysical variable estimated for the given pixel is computed as the mean value of the first n ESUs providing the lowest value of the cost function. Different values of n are considered to get the lowest cost function. This method is reliable only if the ESU NDVI distribution is quite comparable with the whole site NDVI distribution.

Table 1. The methods used by the transfer functions to estimate the biophysical variable values

Therefore, the next processes will not take into account the LUT to estimate the biophysical variable values. The transfer functions will use the REG on reflectance while the REG on logarithm of the reflectance will be the subject of new tests in particular on the forest sites.